In-situ SEM study of fatigue crack growth mechanism in carbon black-filled natural rubber

B Beurrot, Bertrand Huneau, Erwan Verron

In-situ SEM study of fatigue crack growth mechanism in carbon black-filled natural rubber

S. Beurrot, B. Huneau & E. Verron
Institut de Recherche en Génie Civil et Mécanique UMR CNRS 6183,
École Centrale de Nantes, Nantes Cedex, France

ABSTRACT: A micro-tensile testing machine placed in the chamber of a scanning electron microscope is used to perform in-situ fatigue tests on a 43 phr carbon black-filled *cis*-1,4-polyisoprene rubber; the crack tip is observed in realtime during crack propagation. These observations lead to a detailed description of the crack tip morphology, to the understanding of the fatigue crack growth mechanism and to the microstructural explanation of crack branching phenomenon. Finally these results are related to the great fatigue properties of natural rubber and to strain-induced crystallization.

1 INTRODUCTION

Carbon Black-filled Natural Rubber (CB-NR) exhibits longer fatigue life than other elastomeric materials (Beatty 1964). Number of mechanical studies have been proposed to quantify the long-term durability of this material (see Lake (1995, Mars and Fatemi (2002) and the references herein). Nevertheless, only few recent papers investigate the microstructural aspects of fatigue crack growth in rubber (Le Cam et al. 2004; Hainsworth 2007); in these studies, fatigue tests are first conducted until a sufficiently long fatigue crack develops in the sample, then this sample is stretched and the open crack is observed in a Scanning Electron Microscope (SEM). Moreover, Le Cam et al. develop an original "microcutting" technique which permits to observe fatigue damage behind the crack tip and then to propose a scenario of fatigue crack growth in NR (Le Cam et al. 2004).

The aim of the present paper is to verify this previously proposed mechanism and to enrich the understanding of the phenomena involved during fatigue crack growth at the microstructural scale. In this purpose, in-situ SEM fatigue experiments are conducted and crack propagation is observed in real-time. Indeed, we believe that only such observations enable to unquestionably establish the scenario.

The experimental procedure is first described in details. Then, the next section presents the thorough description of the crack tip, clarifies the scenario of crack propagation and explains how secondary cracks appear. Finally, these results are discussed in the light of both macroscopic fatigue properties and straininduced crystallization of natural rubber.

2 EXPERIMENTAL

The aim of the present experiments is to observe the evolution of the crack tip during rubber fatigue crack propagation, in *real-time*. The experiments are conducted in three steps: i. the specimen is precut with a scalpel, ii. a classical fatigue experiment is then conducted in a standard machine until a fatigue crack propagates and iii. the experiment is continued in a micro-tensile testing machine placed in a SEM.

2.1 *Apparatus*

The micro-tensile testing machine used for this study is sufficiently small-sized to be placed in the chamber of a SEM and the double screw driving system leads to easy observation because the centre of the sample, i.e. the position of the crack tip, does not change during loading. Nevertheless, two major difficulties are due to the characteristics of the machine. First, its size and the limited distance between the clamps (from 20 mm to 40 mm) constrain both size and shape of the samples. Indeed, a special design of samples is needed to induce large strain in the vicinity of the crack. Second, as the relative speed of the clamps can vary from 0.1 mm/min to 2 mm/min, the maximum frequency of a fatigue test is 0.83 mHz, such value leading to days-long experiments. This is the reason why samples are pre-cut and the fatigue crack is first propagated in a classical tensile-testing machine.

2.2 *Material and design of the sample*

The material considered here is an industrial 43 phr CB-NR, provided in 2 mm thick calendered sheets.

As mentioned above, a special shape of sample was chosen in order to achieve large strain in crack vicinity and to propagate it; the corresponding geometry is shown in Figure 1.

2.3 *Procedure*

i. The first step consists in pre-cutting the sample to localize the crack in its centre. This cut is made with a scalpel and the resulting crack is less than 1 mm deep and between 1 and 2 mm long.
ii. To reduce the duration of the fatigue experiment, a fatigue crack is initiated from the precut in a standard fatigue machine. Fully relaxing cycles of stretch amplitude 200% are considered and the frequency is chosen to limit self-heating, i.e. less than 1 Hz. This first part of the fatigue test is stopped after the crack has propagated of about 50% of precut deepness.
iii. Finally, the experiment is continued in the small scale tensile machine. Loading conditions are identical to those of ii. except the frequency which is 0.83 mHz. Observation is made in a Jeol 6060LA SEM using secondary electrons imaging. Note that if a too high power electron beam is used, crack tip is damaged: microscopic cracks develop perpendicular to the loading direction. To overcome this difficulty, four parameters need to be lowered to reduce the energy of the electron beam per unit area: the probe current, the accelerating voltage, the magnification and the exposure time. Once these parameters set, the fatigue experiment is stopped once per cycle at maximum stretch to photograph the crack tip.

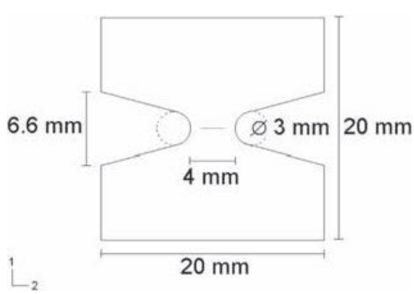

Figure 1. Geometry of samples.

3 MECHANISM OF FATIGUE CRACK PROPAGATION

3.1 *Description of the crack tip*

Figure 2 presents the front view of the fatigue crack tip. In the former figure, tensile direction is indicated by white arrows and the propagation direction is normal to the photomicrograph. As observed previously (Le Cam et al. 2004; Hainsworth 2007), the crack tip is composed of number of diamond-shaped zones separated by ligaments. The pattern of ligaments and diamond-shaped zones can be described as multi-scaled as large diamond-shaped zones delimited by large ligaments are themselves made up of smaller zones delimited by smaller ligaments. The diamond-shaped zones are flat and smooth compared to the ligaments, and those ligaments emerge from the smooth surfaces. The most noticeable characteristic of the crack tip is the pattern regularity. Surprisingly, the ligaments are not parallel to the tensile direction. In fact, they are parallel to two directions which are symmetric with respect to the tensile direction. The angle between the direction of ligaments and the loading direction decreases with the extension of the sample. Consequently, at a given deformation even if the size of diamond-shaped zones varies, all of them have the same length-width ratio. For instance, in Fig. 2, this ratio is 4 to 1. Nevertheless, the size of the diamond-shaped zones is not uniform; indeed the knots of the pattern are not regularly located. Finally, the crack tip also contains another relief feature: as it will be established in

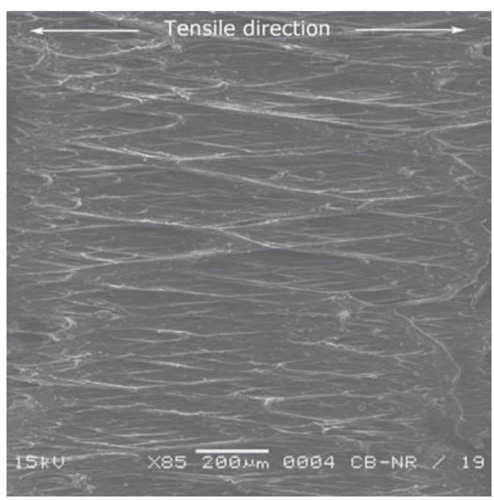

Figure 2. Top view of a representative crack tip.

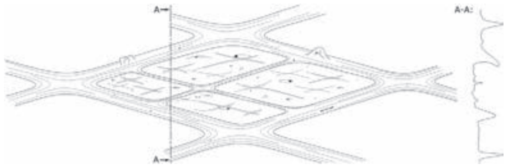

Figure 3. Open crack tip (top view and section).

the following, it corresponds to previously broken and then shrunk ligaments. They are located at the knots of the pattern, i.e. at the intersection of the ligaments.

The previous description was devoted to rubber matrix, but as the material considered in this study is an industrial CB-NR, it contains a lot of different inclusions. Most of them are zinc oxides or carbon black agglomerates. In most of the cases, they are contained in elliptical cavities.

Finally, Figure 3 summarizes the description of the crack tip microstructure: the left-hand drawing shows the front view and presents the different elements described above, and the right-hand drawing is a side view which highlights the relief of the crack front.

3.2 *How does the crack propagate?*

Figure 4 shows six SEM images of a 0.5 mm^2 area of the crack tip taken respectively for the maximum stretch of in-situ fatigue cycles 1, 10, 21, 31 and 41. The micromechanism of fatigue crack growth in rubber can be established thanks to this figure. From one SEM image to another, it clearly appears that all the crack tip zones are affected by crack growth: positions of ligaments change with loading as shown by the white lines drawn on images. It means that the crack front is a surface rather than a line. Moreover, the evolution of the diamond-shaped zones suggests a three-step mechanism for crack propagation as emphasized in Figure 5. In order to describe this evolution, we choose Fig. 5 (a) as the reference state of the zones. Under loading, zones become larger (see changes between Fig. 5 (a), (b) and (c)), and cavities and inclusions appear on the surface (see Fig. 5 (c)). It means that the matter tears and the zone grows deeper in the direction normal to the crack surface, i.e. the direction of crack growth (it cannot be seen in the figure). The more the zone goes deeper, the more the ligaments which delimit it are stretched. Then after a few number of cycles, one of these ligaments breaks (see Fig. 5 (d)) and shrinks (see Fig. 5 (e)). Two different evolutions of the microstructure are observed: a new ligament may emerge or the two diamond-shaped zones

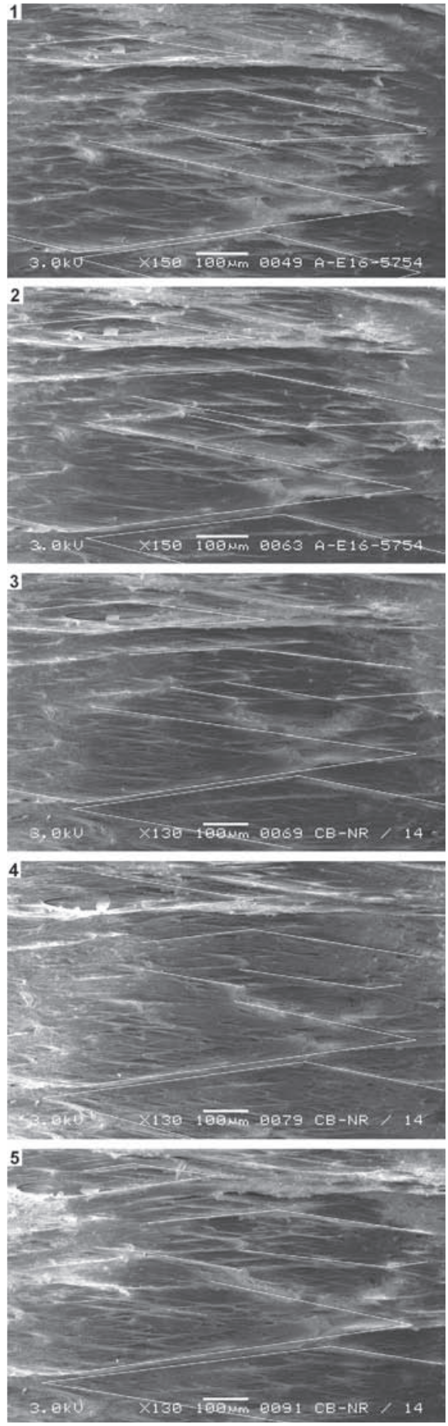

Figure 4. Evolution of a crack tip during cyclic loading after respectively 1, 10, 21, 31 and 41 in-situ cycles.

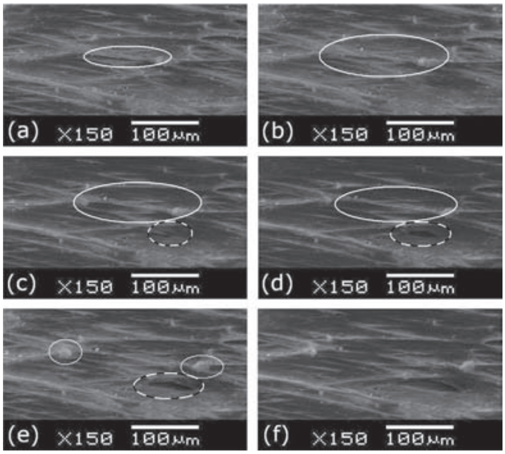

Figure 5. Successive photographs of the same detail of a crack tip during the rupture of a ligament after respectively 1, 3, 4, 5, 6 and 8 in-situ cycles.

separated by the broken ligament may coalesce as shown in Fig. 5 (f). In both cases, the matter reorganizes itself in a large vicinity of the broken ligament through the displacement of ligaments and diamond-shaped zones. In fact, this mechanism repeats itself in every diamond-shaped zone of the crack front. From a temporal point of view, this phenomenon occurs in a continuous manner with different velocities in each point. From a spatial point of view, it can happen simultaneously in different locations of the crack front.

To close this section, we summarize the main elements of the previous mechanism with the help of a five-step scenario as depicted in Figure 6.

a. Fig. 6 (a) presents the initial state of a diamond-shaped zone and its delimiting ligaments; it is a detail of the drawing of the crack tip in Fig. 3,
b. the diamond-shaped zone grows larger and deeper, showing new inclusions and ligaments (see Fig. 6 (b)),
c. as a consequence, ligaments which delimit the zone are stretched and one of them gets thinner than in the previous cycle (see Fig. 6 (c)),
d. eventually, this ligament breaks (see Fig. 6 (d)),
e. finally, the matter reorganizes itself through coalescence of the diamond-shaped zone with one of its neighbours (see Fig. 6 (e)).

3.3 *How do secondary cracks appear?*

In the previous sections, the crack was observed only when opened. However, the study of the closed crack exhibits the path of a fatigue crack in natural rubber. To perform these observations, samples are

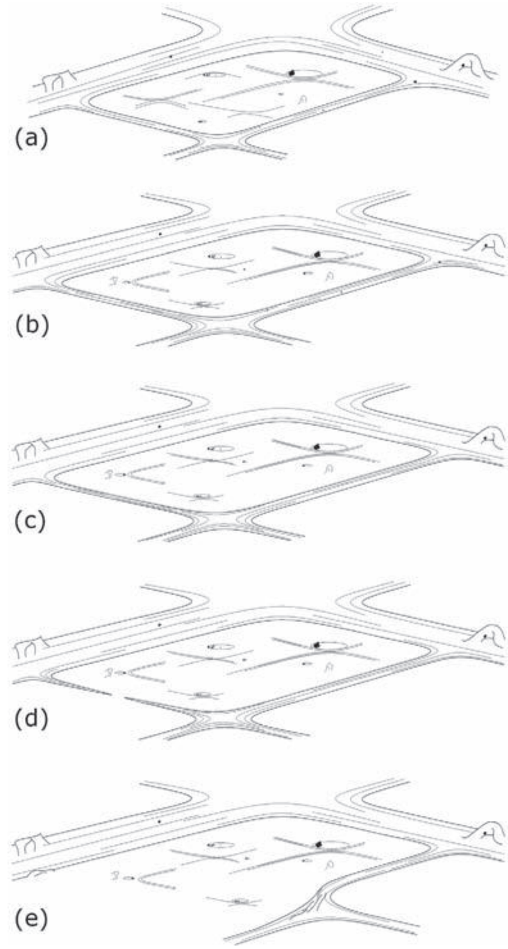

Figure 6. Fatigue crack propagation mechanism.

cut in two with a scalpel along the plane defined by the tensile and propagation directions in the middle of the crack. Figure 7 presents the side view of the crack which is slightly open to observe more easily the crack path. It highlights the main crack path which is normal to the tensile direction and several secondary cracks. Similarly to (Hamed 1994), the term "secondary crack" refers to short deviated cracks developed from the main one. Their length varies from 10 μm to 100 μm. In order to establish the scenario of secondary cracks formation also called "crack branching phenomenon", it is necessary to determine how diamond-shaped zones evolve relatively to the others. In this purpose, the crack tip is observed with a different orientation from the previous images (Figs. 4 and 5): samples are rotated 90° in the SEM chamber to change the orientation of the ligaments with respect to the secondary electron detector. The obtained image is presented in Figure 8; it emphasizes the relief of the crack tip due to the shadow contrast. It shows that all diamond-shaped zones are not in the same plane: some of them are deeper than others (see those indicated by white arrows in Fig. 8).

The crack propagation mechanism proposed in Section 3.2 does not take into account kinetics. The presence of diamond-shaped zones of different deepness in Fig. 8 suggests that even though the diamond-shaped zones evolve in a continuous manner, they do not grow deeper at the same speed. Moreover, recalling that the crack front is a surface rather than a line, the crack branching scenario will be established with the help of Figure 9. It shows the evolution under fatigue loading of three contiguous diamond-shaped zones (*a*, *b*, *c*) located at the crack front surface. It is a simplified representation of the crack tip cross-section: the right-hand drawings describe the close crack with the same view as in Fig. 7 and the left-hand drawings show the same crack but opened. To simplify the discussion, the scenario is established by considering three successive steps:

1. Initially, the three diamond-shaped zones *a*, *b* and *c* are separated by ligaments (grey in the figure) and have the same depth. When the crack is closed, there is only one branch.
2. Later on, when the crack has propagated, zones *a* and *c* have grown deeper than zone *b*. So, the close crack presents two similar branches. The main crack will develop from one or the other (*a* or *c*).

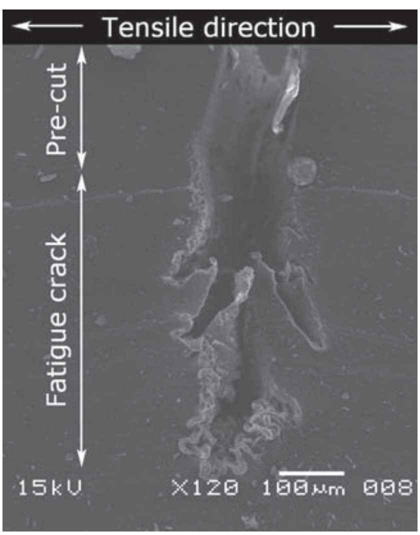

Figure 7. Crack path observed in a cut sample.

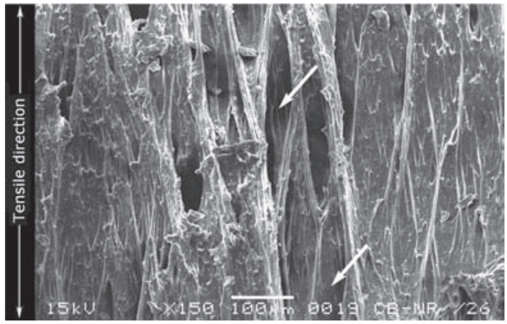

Figure 8. Top view of a crack tip –90° rotated specimen in the chamber of the specimen.

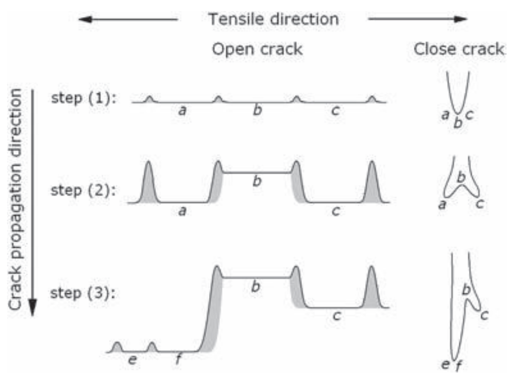

Figure 9. Branching phenomenon mechanism.

3. As the crack continues to propagate, one of the two previous branches will become the main crack due to both local mechanical conditions and microstructure. In the figure, zone *a* has become the main crack, and turned into two new diamond-shaped zones *e* and *f* because the former ligaments which delimited zone *a* broke and new ones appeared; zone *b* does not evolve anymore because it is partially relaxed; and zone *c* forms a secondary crack.

During crack propagation, the elementaryscenario described above repeats: zones *e* and *f* will evolve in the same manner as zones *a*, *b* and *c* in step (1). It is to note, that zones *a*, *b*, *c* can be three single diamond-shaped zones or three groups of several zones.

4 DISCUSSION

Recently, some authors performed interrupted fatigue tests and observed stretched samples in SEM (Le Cam et al. 2004; Hainsworth 2007).

Le Cam et al. observed the damage induced by fatigue and proposed the mechanism of crack propagation in natural rubber. Nevertheless, only observations performed during crack propagation enable to unquestionably establish this mechanism. Here, in-situ SEM experiments have been conducted to observe fatigue crack propagation in rubber in real-time. If such experiments have been already conducted for metallic materials (Crepin et al. 2000), to our knowledge, the present work is the first attempt to apply this technique to rubber materials.

With the careful procedure used during this study, we are able to highly improve the description of both crack tip morphology and propagation mechanism we previously published (Le Cam et al. 2004). First, the crack tip description is enriched: ligaments morphology and orientation were thoroughly investigated. Second, the present mechanism of crack propagation is in good agreement with the previous one, except for the perpendicular micro-cracks and the cavities which were observed by Le Cam et al. and not here. In fact, those micro-cracks were due to the electron beam; moreover, we believe that what was called a cavity in our previous study was only a smooth hollow which deepness was overestimated. Third, additional experiments allow to explain crack branching in NR under fatigue loading conditions.

The microscopic mechanism presented above explains the great fatigue properties of NR at the macroscopic scale: long fatigue life (Mark et al. 2005) and low crack growth rate (Lake 1995; Papadopoulos et al. 2008). Indeed, the ligaments of the crack tip resistto crack propagation in two ways: they induce a surface crack front rather than a tearing line as well as branched cracks which both help to dissipate energy and then hold up crack advance as previously argued by Hamed (Hamed 1994).

The great fatigue properties of NR are usually correlated with its ability to crystallize under deformation. In order to relate this property to our results, we now compare NR to Styrene Butadiene Rubber (SBR), an elastomer which does not exhibit strain-induced crystallization. More precisely, a similar study has been conducted for a SBR material with the same amount of carbon black fillers than in the NR considered here. It highlights three main differences between NR and SBR fatigue crack growth mechanisms:

- SBR crack tip does not present ligaments. Even though we observe sort of filaments parallel to tensile direction, the crack tip is very smooth and experiments reveal that those filaments do not resist to crack propagation as ligaments do in NR,
- the in-situ crack propagation observation also shows that in SBR the crack front is a line rather than a surface as in NR,
- crack branching does not occur in SBR contrary to what is observed in NR.

This comparison demonstrates that the heterogeneity of the microstructure at the crack tip (ligaments, diamond-shaped zones) is a consequence of strain-induced crystallization in NR.

At the close of this study, the mechanism of fatigue crack propagation in NR is qualitatively well-established; further investigations are now required to quantify the heterogeneity of some physical quantities, for example crystallinity and strain, at thecrack tip.

REFERENCES

Beatty, J.R. (1964). Fatigue of rubber. *Rubber Chemistry and Technology 37*, 1341–1364.

Crepin, J., T. Bretheau, D. Caldemaison, and F. Ferrer (2000). Low cycle fatigue behaviour of beta treated zirconium: Partial irreversibility of twinning and consequences for damage. *ActaMaterialia 48*, 505–516.

Hainsworth, S.V. (2007). An environmental scanning electron microscopy investigation of fatigue crack initiation and propagation in elastomers. *Polymer Testing 26*, 60–70.

Hamed, G.R. (1994). Molecular aspects of the fatigue and fracture of rubber. *Rubber Chemistry and Technology 67*, 529–536.

Lake, G.J. (1995). Fatigue and fracture of elastomers. *Rubber Chemistry and Technology 68*, 435–460.

Le Cam, J.B., B. Huneau, E. Verron, and L. Gornet (2004). Mechanism of fatigue crack growth in carbon black filled natural rubber. *Macromolecules 37*, 5011–5017.

Mark, J.E., B. Erman, and F.R. Eirinch (2005). *The Science and Technoloy of Rubber.* Elsevier Inc.

Mars, W.V. and A. Fatemi (2002). A literature survey on fatigue analysis approaches for rubber. *International Journal of Fatigue 24*, 949–961.

Papadopoulos, I.C., A.G. Thomas, and J.J.C. Busfield (2008). Rate transitions in the fatigue crack growth of elastomers. *Journal of Applied Polymer Science 109*, 1900–1910.